Retrieval of kinetic temperature and carbon dioxide abundance from non-local thermodynamic equilibrium limb emission measurements made by the SABER experiment on the TIMED satellite

Christopher J. Mertens *[a], Martin G. Mlynczak[a], Manuel López-Puertas[b], Peter P. Wintersteiner[c], Richard H. Picard[d], Jeremy R. Winick[d], Larry L. Gordley[e], and James M. Russell III[f]

[a]NASA Langley Research Center, Hampton, Virgina, USA
[b]Instituto de Astrofisica de Andalucia, CSIC, Granada, Spain
[c]ARCON Corporation, Waltham, Massachusetts, USA
[d]Air Force Research Laboratories, Hanscom AFB, Massachusetts,USA
[e]G & A Technical Software, Newport News, Virginia, USA
[f]Hampton University, Hampton, Virginia, USA

ABSTRACT

The Sounding of the Atmosphere using Broadband Emission Radiometry (SABER) experiment was launched onboard the TIMED satellite in December, 2001. SABER is designed to provide measurements of the key radiative and chemical sources and sinks of energy in the mesosphere and lower thermosphere (MLT). SABER measures Earth limb emission in 10 broadband radiometer channels ranging from 1.27 μm to 17 μm. Measurements are made both day and night over the latitude range from 54°S to 87°N with alternating hemisphere coverage every 60 days. In this paper we concentrate on retrieved profiles of kinetic temperature (T_k) and CO_2 volume mixing ratio (vmr), inferred from SABER-observed 15 μm and 4.3 μm limb emissions, respectively. SABER-measured limb radiances are in non-local thermodynamic equilibrium (non-LTE) in the MLT region. The complexity of non-LTE radiation transfer combined with the large volume of data measured by SABER requires new retrieval approaches and radiative transfer techniques to accurately and efficiently retrieve the data products. In this paper we present the salient features of the coupled non-LTE T_k/CO_2 retrieval algorithm, along with preliminary results.

Keywords: Remote sensing, non-local thermodynamic equilibrium (non-LTE), thermal structure, carbon dioxide, mesosphere, lower thermosphere, middle atmosphere

1. INTRODUCTION

On December 7, 2001, NASA launched the Sounding of the Atmosphere using Broadband Emission Radiometry (SABER) experiment onboard the TIMED satellite. The satellite was placed in a 74.1 degree inclined, 625 km orbit by a Delta II rocket. The SABER instrument is designed to provide measurements of the major radiative and chemical sources and sinks of energy in the MLT region. The primary science goal of SABER is to achieve major advances in our understanding of the structure, energetics, chemistry, and dynamics of the atmospheric region extending from 60 km to 180 km altitude. This will be accomplished using the measurement approach of spectral broadband emission radiometry. SABER scans the horizon and observes limb emission in 10 broadband spectral channels ranging from 1.27 μm to 17 μm. The observed limb emission profiles are analyzed to provide vertical profiles, with approximately 2 km altitude resolution, of the following parameters: T_k; CO_2, O_3 and H_2O vmr; atomic oxygen and atomic hydrogen; volume emission rates due to $O_2(^1\Delta)$, OH(ν=3,4,5), OH(ν=7,8,9), and NO at 5.3 μm; key atmospheric cooling rates, solar heating rates, chemical heating rates,

* Correspondence: E-mail: c.j.mertens@larc.nasa.gov; Telephone: 757-864-2179; Fax: 757-864-6326

and geotrophic winds. Measurements are made both day and night over the latitude range from 54°S to 87°N with alternating hemisphere coverage every 60 days.

In the MLT region, SABER measures in each channel – with the exception of the 1.27 μm channel, which mainly measures emission from the $O_2(^1\Delta)$ electronic transition – infrared radiation emitted by molecules whose vibration-rotation bands are in non-LTE. Non-LTE kinetic processes and non-LTE radiation transfer complicate the analysis and retrieval of the SABER data products, as well as impose a significant computational burden on data processing. New retrieval approaches and radiation transfer techniques are required to accurately and efficiently retrieve the data products from the large volume of SABER non-LTE emission measurements. In particular, the focus of this paper is on the non-LTE T_k/CO_2 retrieval approach.

Kinetic temperature is retrieved from SABER's broadband measurement of CO_2 15 μm limb emission. This technique was developed more than 30 years ago.[1] In these early experiments, a basic assumption was that CO_2 was well mixed and its volume mixing ratio well known Another key assumption was that the observed CO_2 vibration-rotation bands were in LTE. These assumptions were sufficient for previous sensors whose sensitivity did not permit limb radiance measurements much above 70 km tangent height.

The assumption of LTE in the CO_2 infrared bands and the assumption of uniformly mixed and well known CO_2 vmr, described in the last paragraph, are no longer valid in the MLT region. The variability of CO_2 vmr requires that T_k and CO_2 vmr be retrieved simultaneously. SABER measures CO_2 limb emission in the 15 μm spectral interval to approximately 120 km in altitude for the purpose of determining T_k. SABER also observes 4.3 μm CO_2 limb emission to over 160 km altitude during the day and to approximately 130 km at night. Measurements of CO_2 15 μm and CO_2 4.3 μm limb radiance are combined to retrieve T_k and CO_2 vmr in the MLT region. Non-LTE processes are rigorously accounted for in the retrieval scheme.

Derived profiles of T_k in the MLT are necessary to understand the thermal structure of this region, one of SABER's primary goals. Accurate knowledge of T_k and CO_2 are necessary to quantify the radiative cooling of this region of the atmosphere, largely dominated by infrared emission from the CO_2 15 μm bands. Moreover, T_k is a key input into the retrieval of SABER's other data products. The global distribution of CO_2 is interesting in its own right, as its latitudinal and seasonal variations are not well known and observed, and the mechanism for its departure from its uniformly mixed value is not well characterized.

In a previous work, Mertens et al.[2] presented a non-LTE T_k retrieval algorithm based on observations of CO_2 15 μm broadband limb emission measurements, assuming CO_2 abundance was known. They demonstrated the algorithm using model atmospheres, and studied the sensitivity of retrieved T_k to key atmospheric and kinetic parameters used in the non-LTE CO_2 model. One important conclusion from this work was that CO_2 vmr needed to be known to 15% or better in order to achieve SABER's goal of retrieving T_k to 3 K or better below 100 km. As a result of this study, the non-LTE T_k retrieval algorithm of Mertens et al. has been expanded and updated to enable a simultaneous non-LTE retrieval of T_k and CO_2. In this paper, we present the salient features of the coupled non-LTE T_k/CO_2 retrieval algorithm. The algorithm is demonstrated by showing preliminary retrievals from SABER measurements.

2. RETRIEVAL APPROACH

Kinetic temperature is retrieved in the stratosphere using SABER measured radiance from two CO_2 15 μm channels, a narrow bandpass channel (650-695 cm^{-1}) and a wide bandpass channel (580-760 cm^{-1}). The two CO_2 channels are used to register pressure with altitude in the stratosphere and infer T_k assuming LTE conditions and assuming CO_2 is uniformly mixed and known. This approach is similar to the two-color technique described in Ref..[1] The LTE assumption breaks down in the mesosphere for the infrared CO_2 bands, and CO_2 vmr is no longer uniformly mixed. The simultaneous non-LTE T_k/CO_2 retrieval algorithm is then employed to infer T_k and CO_2 vmr in MLT using measured radiance from the CO_2 15 μm narrow channel and the CO_2 4.3 μm channel (2320-2400 cm^{-1}), respectively.

The LTE-retrieved T_k and pressure described in the preceding paragraph provide the lower boundary conditions for the non-LTE T_k/CO_2 retrieval. The lower boundary condition in the CO_2 vibrational temperature model (described in the next section) is that the source function is given by the Planck function, requiring that

the CO_2 bands are optically thick and in LTE. In the retrieval inversion approach, pressure (p) is obtained by vertically integrating the barometric equation from the lower boundary altitude, requiring that the LTE-retrieved $T_k(p)$ are accurate at the lower boundary altitude. Taking these factors into consideration, the lower boundary altitude of the non-LTE T_k/CO_2 retrieval is nominally taken to be 40 km.

The non-LTE T_k/CO_2 retrieval model is comprised of two main components: (1) the forward radiance model and (2) the inversion model. These two components are described in more detail below.

2.1. Forward Model

The forward radiance model of the retrieval algorithm is the component that simulates the measured radiance along the limb line-of-sight. The forward model itself is composed of two parts: (1) the vibrational temperature model (T_v) and (2) the limb radiance model. Limb radiance is calculated using BANDPAK,[3] now expanded for application to non-LTE calculations.[4] The non-LTE formulation in BANDPAK is a broadband extension of the line-by-line approach described by Edwards et al[5] and initially demonstrated by Mlynczak et al.[6] There are eighteen CO_2 15 μm bands and one O_3 14.1 μm band that contribute to the total limb radiance in the SABER CO_2 15 μm narrow channel spectral bandpass, i.e. above the lower boundary of the non-LTE T_k/CO_2 retrieval model. The SABER 4.3 μm channel has seventeen CO_2 bands that contribute to the total limb radiance at altitudes of approximately 70 km and above. Vibrational temperatures for the nineteen bands that emit in the CO_2 15 μm narrow channel bandpass and the seventeen bands that emit in the CO_2 4.3 μm channel bandpass comprise the non-LTE inputs into the limb radiance model.

The nineteen bands that contribute to the total limb radiance in the SABER CO_2 15 μm narrow channel bandpass can be grouped into seven band-groups: the fundamental ν_2 band of the major (626) isotope (010-626); the fundamental ν_2 bands of the minor (636, 628, and 627) isotopes (010-MIN); the first ν_2 hot bands of the 626 isotope ({020}-626); the first ν_2 hot bands of the minor isotopes ({020}-MIN); the second ν_2 hot bands of the 626 isotope ({030}-626); the O_3 major isotopic ν_2 fundamental band; and the 'remaining' CO_2 bands that contribute to the CO_2 15 μm narrow channel limb radiance. Panels (a) and (b) of Figure 1 show SABER CO_2 15 μm narrow channel limb radiance simulations for the US Standard model atmosphere: limb radiance from the seven band-groups listed above, the total limb radiance, the contribution of each band-group to the total limb radiance, and the noise level (NER: noise equivalent radiance) in the SABER CO_2 15 μm narrow channel. The CO_2 'remainder' band contains contributions from all other CO_2 bands found on the HITRAN 1996 database that are not specified in the band-groups above. Although there are no significant non-LTE effects in the limb radiance from these 'remainder' bands, their cumulative contribution to the total limb radiance is significant and must be modelled, as Figure 1 indicates. The CO_2 'remainder' band is treated as a pseudo-vibrational band – the non-LTE-to-LTE vibrational state population ratios (see Edwards et al.[5]) are set equal to the non-LTE-to-LTE population ratios of the 626 first ν_2 hot band. This step eliminates anomalous thermospheric contributions and guarantees that the correct LTE contributions are included at altitude below approximately 70 km, were their 'true' contribution becomes important, as Figure 1 indicates.

The bands that contribute most to the SABER CO_2 15 μm narrow channel spectral bandpass are the 010-626, {020}-626, and 010-MIN band-groups. The 010-626 band dominates the limb radiance except near 80 km, where the {020}-626 and 010-MIN bands rival, if not exceed, the contribution due to 010-626. The contribution from the other band-groups are much smaller than those mentioned above; however, they must be rigorously modelled in order to retrieve T_k accurately.

Analogous to the discussion of the bands that emit in the SABER CO_2 15 μm narrow channel bandpass, the seventeen bands that contribute to the total limb radiance in the CO_2 4.3 μm channel can be grouped into six band-groups: the fundamental ν_3 band of the 626 isotope (001-626); the fundamental ν_3 bands of the minor isotopes (001-MIN); the first 4.3 μm hot band of the 626 isotope (011-626); and the second, third and fourth 4.3 μm hot bands of the 626 isotope ({021}-626, {031}-626, and {041}-626)). Panels (c) and (d) of Figure 1 for the SABER CO_2 4.3 μm channel are analogous to panels (a) and (b) for the CO_2 15 μm narrow channel. The bands that contribute most to the CO_2 4.3 μm channel radiance are the 001-626, 001-MIN, 011-626, and {021}-626 band-groups. Above 110 km, limb emission in the 4.3 μm channel is dominated by the 001-626 band. Between 95 km and 110 km, the four major band-groups mentioned above are comparable in their contribution

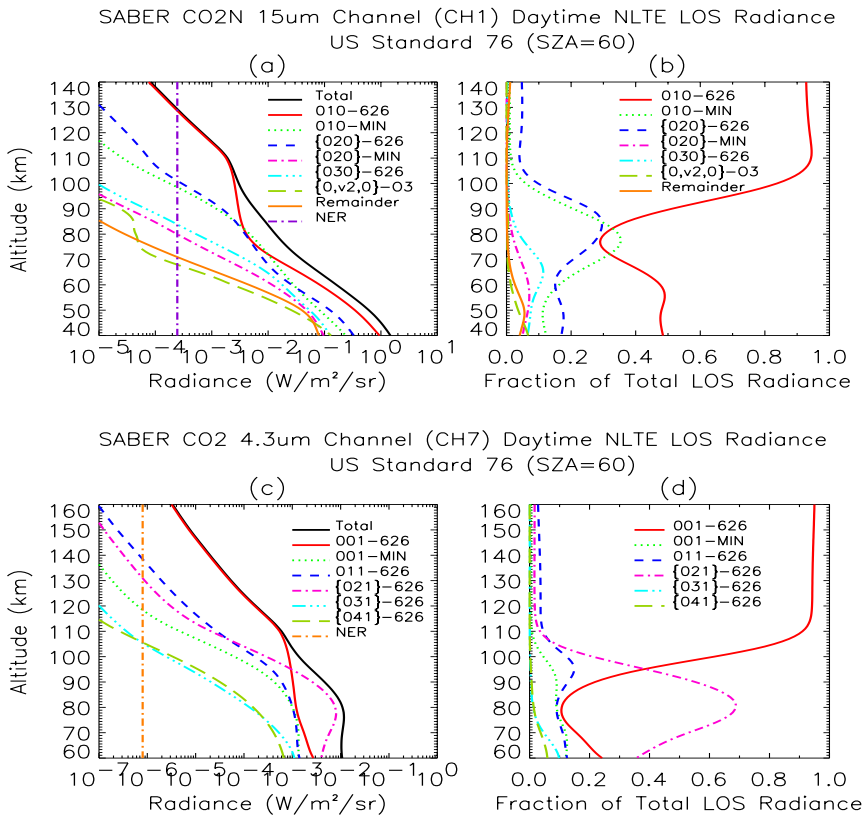

Figure 1. Simulations of daytime (solar zenith angle (SZA) 60 degrees) non-LTE line-of-sight (LOS) limb radiance for the SABER CO_2 15 μm narrow channel (panels (a) and (b)) and CO_2 4.3 μm channel (panels (c) and (d)) for the US Standard atmosphere. See text for details.

to the total limb radiance. Below 95 km, limb emission is dominated by the {021}-626 band-group. However, similar to the case for the SABER CO_2 15 μm narrow channel, all band-groups shown in panels (c) and (d) must be rigorously modelled in order to accurately retrieve CO_2 vmr.

Figure 2 shows a model calculation of the CO_2 T_v's for the US Standard atmosphere. The solar pumped states are shown in panels (a)-(d). The 15 μm T_v's are shown in panel (e). The solar pumped states are responsible for the emission in the SABER CO_2 4.3 μm channel. Furthermore, they have an indirect affect on emission in the CO_2 15 μm channel through collisional and radiative coupling to the CO_2 ν_2 vibrational state manifold, as indicated in panel (f). The vibrational temperatures are calculated from the operational CO_2 T_v model, which is based on the Modified Curtis Matrix approach advanced by López-Puertas et al..[7] The operational CO_2 T_v model uses BANDPAK to perform all the radiation transfer calculations and will be described in more detail in Refs.[4] and.[8]

2.2. Inversion Method

Kinetic temperature and CO_2 vmr are retrieved by successively iterating between two independent retrieval modules: one for $T_k(p)$, assuming CO_2 is known, and the other one for CO_2 vmr, assuming $T_k(p)$ is known. The iteration stops when successive CO_2 profiles have relaxed sufficiently over the altitude range of the non-LTE retrieval model. The global convergence criteria for the coupling between the T_k and CO_2 retrievals is that the average difference between two successive CO_2 vmr retrievals, i.e., averaged over all the retrieved tangent levels, does not exceed a user-specified percentage. Retrieval simulations for various model atmospheres (US

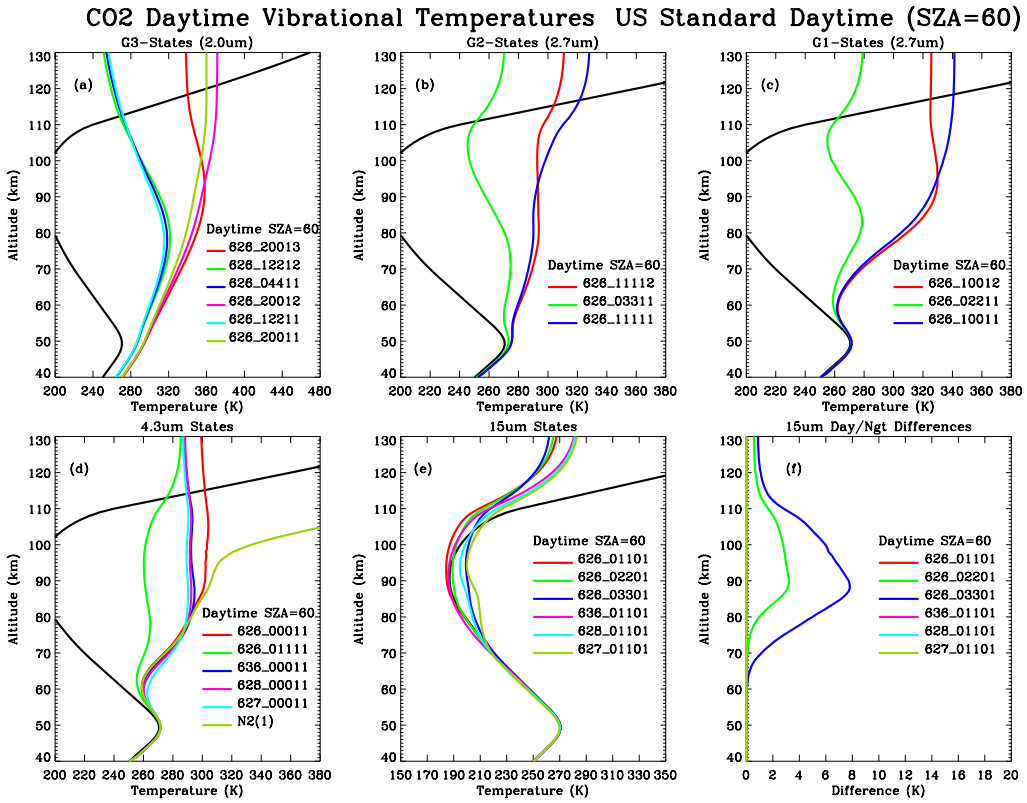

Figure 2. Simulations of daytime (solar zenith angel (SZA) 60 degrees) CO_2 vibrational temperatures for US Standard atmosphere. See text for details.

Standard, Polar Summer, and Polar Winter) have shown that the differences between the last and next-to-the-last retrieved CO_2 profiles are small enough not to significantly affect an additional T_k retrieval; thus, justifying the termination of the non-LTE T_k/CO_2 retrieval algorithm based on the convergence of the CO_2 profile. Below we briefly describe the separate T_k and CO_2 retrieval modules. A detailed algorithm description will appear elsewhere.[9]

First we describe the non-LTE T_k retrieval module. There are two primary relaxation loops. In the inner loop, a T_k profile is retrieved using the onion-peel approach while pressure, CO_2 vmr, and the T_v's are held fixed. Kinetic temperature is retrieved at each tangent altitude by adjusting the local T_k until the modelled radiance matches the measured radiance within the convergence criterion. The temperature is adjusted using the Levenberg-Marquardt method.[10] The inner loop convergence criterion is a requirement that the difference between successive iterations is much less than the expected errors in the solution.[11] The fraction of the solution error required to satisfy the convergence criterion is user-specified.

The onion-peel approach is critical to retrievals from CO_2 limb emission measurements in the MLT region, since the CO_2 15 μm limb radiance for mesospheric tangent heights is dominated by emission from higher altitude layers.[12] The same is also true for CO_2 4.3 μm limb radiance. The onion-peel technique ensures that the modelled emission matches the measured radiance from the upper altitude layers, even though the retrieved temperature-pressure-CO_2 combination may be incorrect at intermediate steps in the relaxation process. For a particular limb path, the effect is greater sensitivity to the local T_k at the sought-after tangent altitude.

In the outer relaxation loop, the pressure profile is rebuilt from the lower boundary altitude using the onion-peel retrieved T_k profile and the barometric pressure law. The vibrational temperatures are updated using the CO_2 T_v model with the previously retrieved T_k, CO_2 vmr, and pressure profile as input. The onion-peel retrieval (inner loop) is repeated until the entire inferred T_k profile relaxes within the convergence criterion,

which is a requirement that the retrieved temperature profile differences between two successive onion-peel retrieval iterations be much smaller than the expected solution error at all tangent heights above the lower boundary altitude.

Next we describe the non-LTE CO_2 vmr retrieval module. Because of the severe nonlinearities in the radiation transfer along the limb line-of-sight in the SABER CO_2 4.3 μm channel bandpass, the CO_2 vmr retrieval module is composed of a juxtaposition of two retrieval approaches. The first approach is the nonlinear relaxation method of Twomey-Chahine,[13] modified here for limb path geometry and broadband radiance measurements. In the current approach, the kernel function, or weighting function, is the contribution of each layer along the limb line-of-sight to the total limb radiance, divided by the layer-averaged CO_2 abundance. Similar to the non-LTE T_k retrieval, the CO_2 vmr is retrieved at each tangent altitude using the onion-peel method. The convergence criterion was described in the first paragraph of this section. If the criterion is not satisfied, the non-LTE T_k retrieval is repeated, followed by a subsequent CO_2 vmr retrieval using the modified Twomey-Chahine approach. Once the global convergence criterion is satisfied, one final CO_2 vmr retrieval is performed using the Levenberg-Marquardt approach, analogous to the inner loop relaxation scheme of the non-LTE T_k retrieval described above.

The nonlinearities in the CO_2 4.3 μm radiation transfer are too severe to use a retrieval algorithm based on Newtonian iteration, applicable to weakly nonlinear problems,[14] or a Levenberg-Marquardt approach, applicable to moderately nonlinear problems.[14] Consequently, the nonlinear relaxation method of Twomey-Chahine is used to infer CO_2 vmr in the coupled non-LTE T_k/CO_2 retrieval algorithm. However, optimal estimation approaches, such as the Levenberg-Marquardt approach, provide useful statistical information: the estimated solution error, quality metrics such as the χ^2, or penalty, function, and more theoretical-based convergence criterion. Therefore, the final CO_2 vmr retrieval uses the Levenberg-Marquardt algorithm to refine the modified Twomey-Chahine approach and provide the useful statistical information described above.

3. RESULTS AND DISCUSSION

In this section we present preliminary non-LTE T_k/CO_2 retrievals from SABER observations. There are a number of additional atmospheric parameters required as input into the CO_2 T_v model: O_2, N_2, $O(^3P)$, and $O(^1D)$, for example. In the preliminary retrieved profiles shown in this section, the atmospheric parameters listed above were obtained from the TIMED-GCM climatology produced for SABER analysis.

Figure 3 shows nighttime non-LTE T_k retrievals on March 3, 2002, near 69°N. The retrieved T_k profiles are compared to the Lübken and von Zahn[15] climatological monthly mean T_k profile for March. The monthly mean profile was generated from T_k measurements taken from sodium lidar, falling spheres, and rocketborne mass spectrometer and ionization gauge measurements (see Ref.[15] for details). Between 60 km and 105 km, the differences between the individual SABER-derived T_k profiles and the monthly mean profile are within the natural variability in the monthly mean T_k profile for March at 69°N.[15] Below 60 km the SABER T_k profiles are substantially cooler than the climatological mean; above 105 km the SABER T_k profiles are substantially warmer than the climatological mean. Further analysis is required to understand these differences.

The following figures demonstrate the coupled non-LTE T_k/CO_2 retrieval algorithm for daytime SABER observations. Figure 4 shows retrieved CO_2 profiles on January 28 and March 3, 2002. For each day, retrieved profiles are shown at latitudes of approximately 44°N and 27°S. The retrieved profiles are shown as solid lines. Climatological mean CO_2 profiles from the TIMED-GCM model are shown as dashed lines[16] – which most closely correspond to the time, season and geo-location of the SABER measurements.

For equinox conditions, model simulations indicate that the latitudinal distribution of CO_2 is symmetrically distributed about the equator (see Ref.[17] and references therein). Consequently, the CO_2 profiles for March 3 at 44°N and 27°S should be very similar, as Figure 4 indicates. However, SABER-derived CO_2 profiles suggest a much larger depletion of CO_2 in the upper mesosphere and lower thermosphere than predicted by the TIMED-GCM model and previous rocket borne mass spectrometer measurements,[17] similar to the findings of other recent CO_2 retrievals from infrared emission measurements (see Refs.,[18] ,[19] and[20]). From Figure 4, the TIMED-GCM simulations predict that for equinox conditions, the CO_2 abundance for 27°S is greater than

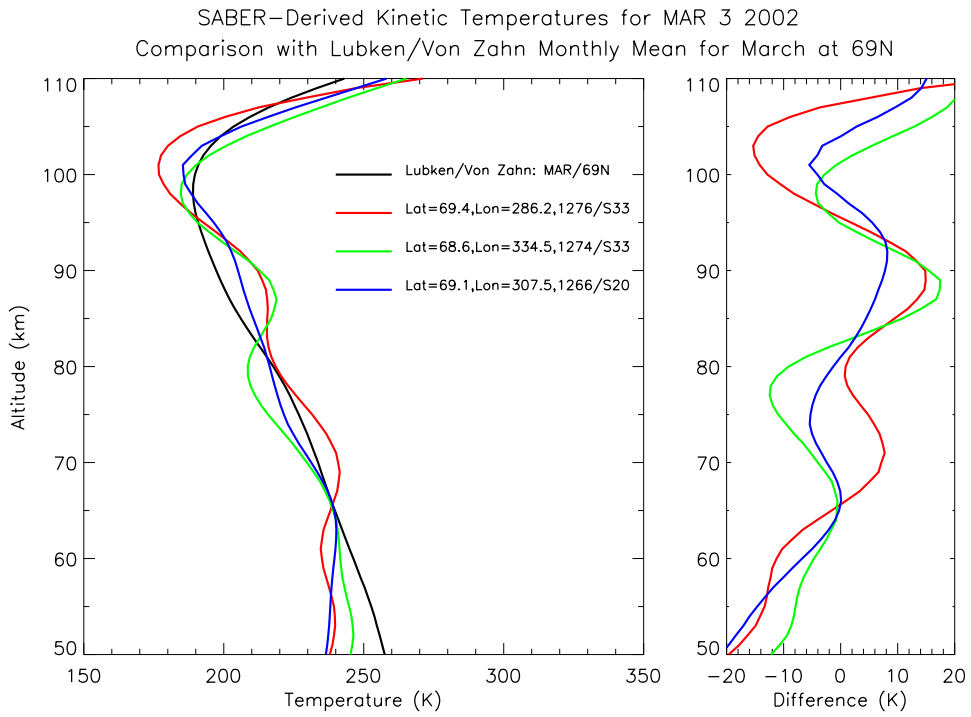

Figure 3. Nighttime non-LTE T_k retrievals from SABER measurements on March 3, 2002, near 69°N. The latitude, longitude, orbit and scan numbers, respectively, for the SABER measurements are indicated in the legend. The retrieved T_k profiles are compared to the climatological monthly mean March T_k profile from Lubken and von Zahn.[15]

the CO_2 abundance for 44°N above 100 km. The SABER retrievals show just the opposite effect: the CO_2 abundance at 27°S is significantly depleted relative to the CO_2 abundance at 44°N.

Model simulations indicate that for solstice conditions, CO_2 vmr remains constant up to higher altitudes in the summer hemisphere and departs from its constant value at lower altitudes in the winter hemisphere; an effect governed by upward transport in the summer hemisphere and downward transport in the winter hemisphere.[17] SABER CO_2 retrievals support this conclusion, as indicated in Figure 4 for the January 28 profiles. However, the retrieved CO_2 profile at 44°N is significantly depleted with respect to the corresponding TIMED-GCM profile, while the corresponding TIMED-GCM profile for the 27°S measurement seems to fit the measurement scenario quite well.

Figure 5 shows the T_k profiles that were retrieved simultaneously with the CO_2 profiles shown in the previous figure. Similar to Figure 4, retrieved profiles are shown on January 28 and March 3, 2002, at approximately 44°N and 27°S. Retrieved profiles are shown as solid lines and TIMED-GCM climatological mean T_k profiles are shown as dashed lines – which correspond most closely to the time, season and geo-location of the SABER measurements.

The most noticeable features in Figure 5 above 110 km are found in the T_k profiles for January 28 and March 3 at 44°N. There's an inversion layer in the January 28 profile and T_k decreases with increasing altitude in the March 3 profile. Neither of these features are real; rather, they're due to large noise spikes in the CO_2 15 μm narrow channel radiance profiles. In general, measurement noise will prohibit reasonable T_k retrievals much above 110 to 115 km.

The SABER-derived T_k profiles in Figure 5 show a great deal of vertical wave structure, suggestive of rather strong tidal signatures. The SABER T_k profiles are generally warmer than the TIMED-GCM profiles between

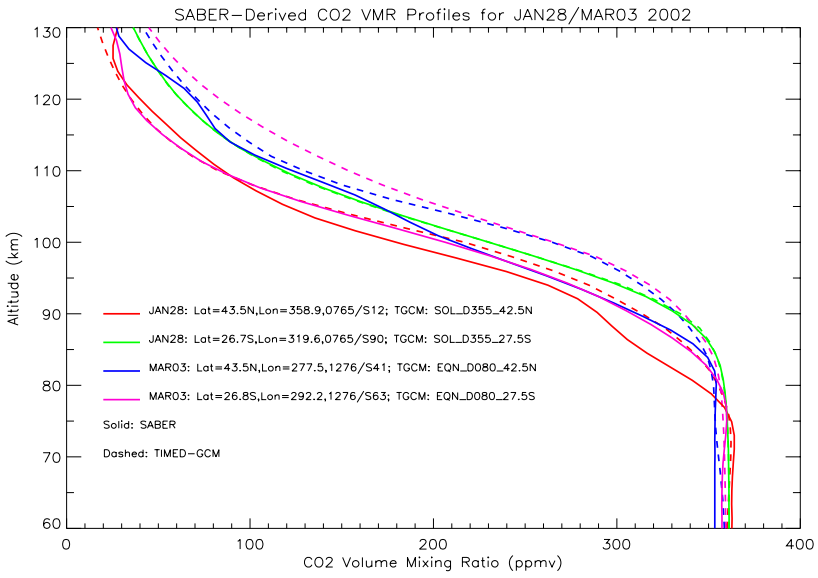

Figure 4. Daytime non-LTE T_k/CO_2 retrievals from SABER measurements on January 28 and March 3, 2002. In this figure we show the retrieved CO_2 profiles. The month, day, latitude, longitude, orbit and scan numbers, respectively, for the SABER measurements are indicated in the legend. The retrieved CO_2 profiles are compared to the TIMED-GCM climatological mean that most closely corresponds to the SABER measurement time, season and geo-location. The TIMED-GCM profiles shown were computed for two time periods: daytime winter solstice (indicated by SOL_D355) and daytime spring equinox (indicated by EQN_D080).

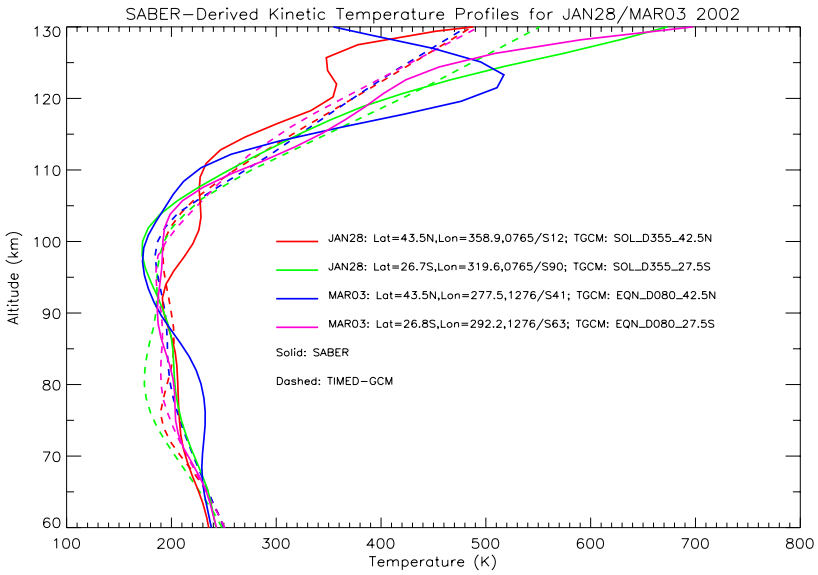

Figure 5. Daytime non-LTE T_k/CO_2 retrievals from SABER measurements on January 28 and March 3, 2002. In this figure we show the retrieved T_k profiles. The month, day, latitude, longitude, orbit and scan numbers, respectively, for the SABER measurements are indicated in the legend. The retrieved T_k profiles are compared to the TIMED-GCM climatological mean that most closely corresponds to the SABER measurement time, season and geo-location. The TIMED-GCM profiles shown were computed for two time periods: daytime winter solstice (indicated by SOL_D355) and daytime spring equinox (indicated by EQN_D080).

70 km and 90 km. In particular, the January 28 profile at 27°S and the March 3 profile at 44°N are significantly warmer than the model profiles between 70 km and 90 km. On the other hand, the SABER T_k profile for March 3 at 27°S is reasonably close to the corresponding TIMED-GCM profile below 110 km. The SABER January 28 profile at 44°N has a feature that resembles a double mesopause region at approximately 93 km and 110 km. The corresponding model profile has a double mesopause at approximately 75 km and 100 km. For all the profiles shown in Figure 5, the SABER T_k profiles are cooler than the TIMED-GCM profiles below approximately 65 km.

4. CONCLUSIONS

In this paper we briefly described the coupled non-LTE T_k/CO_2 retrieval algorithm used to infer T_k and CO_2 vmr from limb emission measurements observed from SABER's CO_2 15 μm and CO_2 4.3 μm broadband radiometer channels. We have shown preliminary T_k/CO_2 profiles from SABER observations. The preliminary results look reasonable. Nighttime T_k retrievals near 69°N generally compare favorably with the Lübken and von Zahn climatology. Daytime T_k retrievals compare reasonably well with TIMED-GCM profiles, although some of the SABER T_k profiles seem to be modulated by quite large tidal signatures. Retrieved CO_2 vmr profiles seem to confirm that models (e.g., TIMED-GCM) tend to overpredict CO_2 in the MLT region.

At the time of this writing, a number of instrument corrections are being made to improve the overall quality of the SABER radiance measurements. The non-LTE T_k/CO_2 retrieval algorithm presented here is currently being interfaced and ingested into the overall SABER software system. In the near future, a number of important atmospheric input parameters (i.e., input into the CO_2 T_v model) will be derived below 100 km from SABER observations – for example, $O(^3P)$ and $O(^1D)$. Thus, the excellent quality of the SABER measurements combined with the non-LTE T_k/CO_2 retrieval algorithm presented here, and along with the other SABER non-LTE retrievals algorithms, offer the potential to significantly improve our understanding of the MLT thermal structure, chemistry, and energetics.

ACKNOWLEDGMENTS

M.L-P. has been partially supported by MCYT under contracts PNE-017/2000-C and REN2001-3249. RHP and and JRW are grateful to Kent Miller of the Air Force Office of Scientific Research for partial support of this work. The work of PPW was carried out under contract to Air Force Research Laboratories under contract F19628-96-C-0048. All authors acknowledge support from NASA Langley under its SABER project.

REFERENCES

1. J. C. Gille and F. B. House, "On the inversion of limb radiance measurments. I: Temperature and thickness", *J. Atmos. Sci.* **28**, pp. 1427-1442, 1971.
2. C. J. Mertens, M. G. Mlynczak, M. López-Puertas, P. P. Wintersteiner, R. H. Picard, J. R. Winick, L. L. Gordley, and J. M. Russell III, "Retrieval of mesospheric and lower thermospheric kinetic temperature from measurements of CO_2 15 μm Earth limb emission under non-LTE conditions", *Geophys. Res. Lett.*, **28**, pp. 1391-1394, 2001.
3. B. T. Marshall, L. L. Gordley, and D. A. Chu, "BANDPAK: Algorithms for modeling broadband transmission and radiance", *J. Quant. Spectrsc. Radiat. Transfer* **52**, pp. 581-599, 1994.
4. C. J. Mertens, M. G. Mlynczak, M. Lópes-Puertas, P. P. Wintersteiner, R. H. Picard, J. R. Winick, B. T. Marshall, L. L. Gordley, and J. M. Russell III, "Line-by-line and broadband non-LTE radiation transfer algorithms for the operational processing of satellite data", *manuscript in preparation.*
5. D. P. Edwards, M. López-Puertas, and M. A. López-Valverde, "Non-LTE thermodynamic equilibrium studies of the 15-μm bands of CO_2 for atmospheric remote sensing", *J. Geophys. Res.* **98**, pp. 14,955-14,977, 1993.
6. M. G. Mlynczak, D. S. Olander, and M. López-Puertas, "Rapid computation of spectrally integrated non-LTE limb emission", *J. Geophys. Res.* **99**, pp. 25,761-25,772, 1994.

7. M. López-Puertas, G. Zaragoza, M. A. López-Valverde, and F. W. Taylor, "Non local thermodynamic equilibrium (LTE) atmospheric limb emission at 4.6 μm. 1. An update of the CO_2 non-LTE radiation tranfer model", *J. Geophys. Res.*, **103**, pp. 8499-8513, 1998.
8. P. P. Wintersteiner, M. López-Puertas, C. J. Mertens, R. H. Picard, and J. R. Winick, "Comparison of three algorithms for evaluating non-LTE populations of CO_2 states in the middle atmosphere", *manuscript in preparation.*
9. C. J. Mertens, M. G. Mlynczak, M. López-Puertas, P. P. Wintersteiner, R. H. Picard, J. R. Winick, L. L. Gordley, and J. M. Russell III, "Simultaneous retrieval of temperature and CO_2 abdundance from measurements of CO_2 15 μm and 4.3 μm earth limb emission measurements under non-LTE conditions: Algorithm description and results", *manuscript in preparation.*
10. W. H. Press, S. A. Teukolsky, W. T. Vetterling, and B. P. Flannery, *Numerical Recipes in Fortran*, Second Edition, p. 678, Cambridge University Press, New York, 1992.
11. C. J. Marks and C. D. Rodgers, "A Retrieval Method for Atmospheric Composition From Limb Emission Measurements", *J. Geophys. Res.*, **98**, pp. 14,939-14,953, 1993.
12. P. P. Wintersteiner, R. H. Picard, R. D. Sharma, J. R. Winick, and R. A. Joseph, "Line-by-line radiative excitation model for the non-equilibrium atmosphere: Application to CO_2 15-μm emission", *J. Geophys. Res.*, **97**, pp. 18,083-18,117, 1992.
13. S. Twomey, B. Herman, and R. Rabinoff, "An Extension of the Chahine Method of Inverting the Radiation Transfer Equation", *J. Atmos. Sci.*, **34**, pp. 1085-1090, 1977.
14. C. D. Rodgers, *Inverse Methods for Atmospheric Sounding: Theory and Practice*, World Scientitic, 2000.
15. F. -J. Lüken and U. von Zahn, "Thermal Structure of the Mesopause region at Polar Latitudes", *J. Geophys. Res.*, **96**, pp. 20,841-20,857, 1991.
16. R. G. Roble, "On the feasibility of developing a global atmospheric model extending from the ground to the exosphere", *Atmospheric Science Across the Stratopause*, Geophysical Monograph 123, American Geophysical Union, 2000.
17. M. López-Puertas, M. Á. López-Valverde, R. R. Garcia, and R. G. Roble, "A review of CO_2 and CO abundances in the middle atmosphere", *Atmospheric Science Across the Stratopause*, Geophysical Monograph 123, American Geophysical Union, pp.83-100, 200.
18. M. López-Puertas, G. Zaragoza, M. Á. López-Valverde, and F. W. Taylor, "Non local thermodynamic equilibrium (LTE) atmospheric limb emission at 4.6 μm 2. An analysis of the daytime wideband radiances as measured by UARS improved stratospheric and mesospheric sounder", *J. Geophys. Res.*, **103**, pp. 8515-8530, 1998.
19. G. Zaragoza, M. López-Puertas, M. Á. López-Valverde, and F. W. Taylor, "Global distribution of CO_2 in the upper mesosphere as derived from UARS/ISAMS measurements", *J. Geophys. Res.*, **105**, pp. 19,829-19,839, 2000.
20. M. Kaufmann, O. A. Gusev, K. U. Grossmann, R. G. Roble, M. E. Hagan, and C. Hartsough, and A. A. Kutepov, "The vertical and horizonal distribution of CO_2 densities in the upper meosphere and lower thermosphere as measured by CRISTA", *accepted by J. Geophys. Res.*